### Title
Variable North Pacific influence on drought in southwestern North America since AD 854




### Journal
Nature Geoscience, 6(8)

### ISSN
1752-0894



### Authors
McCabe-Glynn, Staryl
Johnson, Kathleen R
Strong, Courtenay
et al.



### Publication Date
2013-08-01

### DOI
10.1038/ngeo1862

Peer reviewed

nature geoscience

LETTERS

PUBLISHED ONLINE: 7 JULY 2013 | DOI: 10.1038/NGEO1862

# Variable North Pacific influence on drought in southwestern North America since AD 854

Staryl McCabe-Glynn[1], Kathleen R. Johnson[1]*, Courtenay Strong[2], Max Berkelhammer[3], Ashish Sinha[4], Hai Cheng[5,6] and R. Lawrence Edwards[5]

**Precipitation in southwestern North America has exhibited significant natural variability over the past few thousand years[1]. This variability has been attributed to sea surface temperature regimes in the Pacific and Atlantic oceans, and to the attendant shifts in atmospheric circulation patterns[1,2]. In particular, decadal variability in the North Pacific has influenced precipitation in this region during the twentieth century[3,4], but links to earlier droughts and pluvials are unclear. Here we assess these links using $\delta^{18}O$ data from a speleothem from southern California that spans AD 854–2007. We show that variations in the oxygen isotopes of the speleothem correlate to sea surface temperatures in the Kuroshio Extension region[5] of the North Pacific, which affect the atmospheric trajectory and isotopic composition of moisture reaching the study site. Interpreting our speleothem data as a record of sea surface temperatures in the Kuroshio Extension, we find a strong 22-year periodicity, suggesting a persistent solar influence[6] on North Pacific decadal variability. A comparison with tree-ring records of precipitation[1] during the past millennium shows that some droughts occurred during periods of warmth in the Kuroshio Extension, similar to the instrumental record[4]. However, other droughts did not and instead must have been influenced by other factors. Finally, we find a significant increase in sea surface temperature variability over the past 150 years, which may reflect an influence of greenhouse gas concentrations on variability in the North Pacific.**

Precipitation in southwestern North America (SWNA) is highly seasonal and exhibits interannual to multidecadal variability linked to naturally recurring large-scale atmospheric circulation patterns. Instrumental records and climate model simulations demonstrate that Pacific sea surface temperature (SST) patterns related to coupled climate modes such as the El Niño/Southern Oscillation (ENSO) and the Pacific Decadal Oscillation (PDO) exert substantial control on SWNA hydroclimate over the twentieth century, with typically drier conditions during the cool phases (negative PDO and La Niña) and wetter conditions during the warm phases (positive PDO and El Niño)[1,3,7]. Furthermore, North Atlantic SSTs also played a role in twentieth-century droughts, with warmer SSTs linked to drier conditions[2,4]. SST reconstructions, however, provide conflicting evidence about the cause of earlier droughts. For instance, the SWNA megadroughts of the Medieval Climate Anomaly (MCA) have been attributed to persistent La Niña-like conditions[1,8,9], but interannual mechanisms such as ENSO may not be appropriate for explaining decadal- to centennial-scale precipitation variability. Although many reconstructed droughts of the past millennium do seem synchronous with cool eastern equatorial Pacific (EEP) SSTs, others do not[10,11], thus highlighting the potential importance of other influences such as the North Pacific and the North Atlantic.

Most climate models project enhanced aridity in SWNA as a result of global warming[12]. The projected drying trend is attributed to decreased winter precipitation as a result of a strengthening and poleward shift of the North Pacific storm track. However, given the strong influence of the Pacific Ocean on SWNA hydroclimate, the magnitude and extent of drought will be strongly dependent on the specific SST patterns that result from radiative forcing and natural decadal variability[12]. Despite the fact that North Pacific decadal variability (NPDV) is a critical predictor of regional and global climate change, twentieth century simulations with Intergovernmental Panel on Climate Change Fourth Assessment Report models show little agreement with observations of the two leading North Pacific SST patterns, the PDO and the North Pacific Gyre Oscillation[13]. This reflects significant uncertainty about the mechanisms of NPDV, with several studies suggesting that NPDV is the low-frequency manifestation of tropical ENSO variability[14], whereas other studies suggest that mid-latitude ocean–atmosphere coupling dominates[15]. Improved understanding of the dynamics of decadal-scale SST variability, tropical–North Pacific teleconnections, and the past response to changing boundary conditions is therefore critical for predicting future NPDV, yet progress is limited at present by the paucity of high-resolution palaeoclimate records. Existing records of North Pacific SSTs over the past millennium are primarily PDO reconstructions derived from tree rings that assume a consistent response of regional precipitation to NPDV (refs 16–18) and are influenced by multiple factors including temperature and evapotranspiration. These factors, variations in the spatial patterns of drought, and the potential nonlinear response of tree growth to moisture availability may explain why there is only weak coherence among independent PDO reconstructions before the twentieth century[19]. Here, we use a new speleothem-based approach to reconstruct North Pacific SSTs by taking advantage of the strong relationship between oxygen isotopes in precipitation in SWNA and North Pacific storm trajectories[20,21].

We have developed an absolute-dated, high-resolution $\delta^{18}O$ record from a stalagmite, CRC-3, collected from Crystal Cave in Sequoia National Park, California (36.59° N; 118.82° W; 1,386 m; Supplementary Fig. S1). The record is based on 1,054 $\delta^{18}O$ measurements (Supplementary Fig. S2) conducted on samples

[1]Department of Earth System Science, University of California, Irvine, California 92697, USA, [2]Department of Atmospheric Sciences, University of Utah, Salt Lake City, Utah 84112, USA, [3]CIRES/ATOC, University of Colorado, Boulder, Colorado 80309, USA, [4]Department of Earth Science, California State University, Dominguez Hills, Carson, California 90747, USA, [5]Department of Earth Sciences, University of Minnesota, Minneapolis, Minnesota 55455, USA, [6]Institute of Global Environmental Change, Xi'an Jiaotong University, Xi'an 710049, China. *e-mail: kathleen.johnson@uci.edu

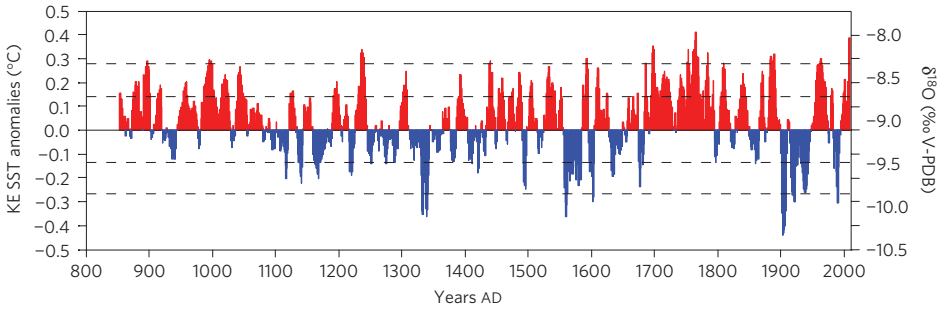


**Figure 1 | Extended Kuroshio Extension SST anomaly reconstruction and CRC-3 $\delta^{18}O$ values.** SST anomalies were calculated using a linear regression of low-pass-filtered SST anomalies within the Kuroshio Extension (KE) region and the CRC-3 $\delta^{18}O$ time series over the full period of overlap (1857–2007). Positive values (red) indicate warmer SSTs and negative values (blue) indicate cooler SSTs compared with the long-term mean. Dashed lines show 1 and 2 standard deviations (0.14 and 0.28 °C), respectively.

micromilled from the 10.4-cm-long stalagmite (Supplementary Table S1). The age model for CRC-3, which extends from AD 854–2007 (Supplementary Fig. S3) is based on ten $^{230}Th$–$^{234}U$ dates (Supplementary Table S2) and a top age of AD 2007, the time when a glass plate was placed over the stalagmite to confirm active calcite precipitation. The model was developed using the StalAge algorithm, which allows robust uncertainty estimation throughout the length of the record[22]. To further constrain the age model over the twentieth century, we conducted 34 radiocarbon measurements on CRC-3 to locate the $^{14}C$ bomb peak. Results show that $\Delta^{14}C$ begins to rise at approximately AD 1955, synchronous with or slightly lagging the atmosphere. This is consistent with the rapid transmission of bomb $^{14}C$ observed at other sites[23] and thus provides support for the StalAge model (Supplementary Discussion and Fig. S4). Cave monitoring data suggest that the CRC-3 calcite formed under isotopic equilibrium conditions and that the $\delta^{18}O$ primarily reflects interannual changes in the $\delta^{18}O$ of precipitation above the cave (Supplementary Discussion).

Previous research indicates that the isotopic composition of precipitation in southern California is largely determined by the storm track delivering precipitation to this region[20]. To further investigate this, we conducted trajectory and clustering analysis and measured the isotopic composition of precipitation from storms reaching the study area between AD 2001 and 2005. Our analysis shows three primary clusters of storms entering the region, with the lowest $\delta^{18}O$ precipitation arriving from the North Pacific and the highest from the tropical Pacific (Supplementary Fig. S5). Although some isotopic variability may arise from local conditions, these effects are most likely to enhance the proxy response. For instance, during the twentieth century, periods of warm Kuroshio Extension SSTs are associated with cool SSTs off the California coast[5,15] and increased aridity in SWNA (ref. 4); hence, the signal due to increased transport of isotopically enriched moisture during these periods may be amplified by decreased near-surface relative humidity and/or decreased rainfall, which also tend to increase precipitation $\delta^{18}O$ (ref. 21).

The trajectory of storms arriving in SWNA is strongly dependent on Pacific SST patterns[24], which influence the position of the high- and low-pressure centres in the North Pacific and over the North American continent. An inverse correlation with the PDO Index[7] between 1925 and 2008 ($r = -0.43, p = 0.04$) suggests that CRC-3 $\delta^{18}O$ values are sensitive to North Pacific SST patterns. To examine the underlying physical ocean–atmosphere mechanisms through which North Pacific SSTs may impact this record, we investigated SST anomalies[25] associated with the CRC-3 $\delta^{18}O$ values (Fig. 2a and Supplementary Fig. S6). High $\delta^{18}O$ values are strongly associated with anomalously warm SSTs in the Kuroshio Extension region east of Japan (white outline, Fig. 2a; essentially the PDO's western centre of action) whereas the corresponding

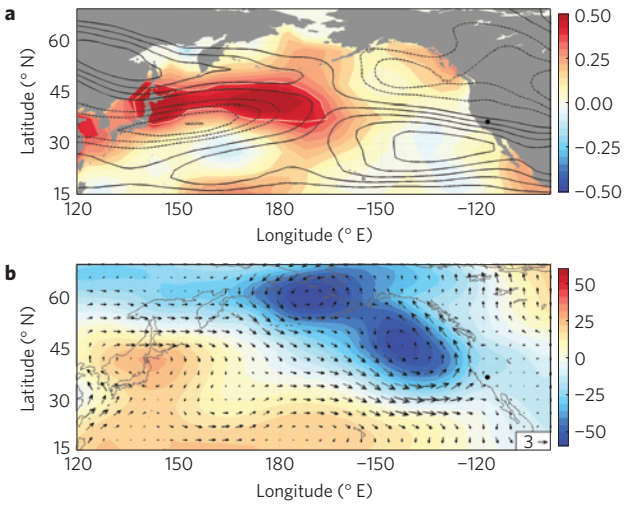


**Figure 2 | SST, wind and geopotential heights associated with CRC-3 $\delta^{18}O$ anomalies.** All results show the mean from years in the upper quartile of $\delta^{18}O$ minus the mean of years in the lower quartile of $\delta^{18}O$. The black dot shows the Crystal Cave location. **a**, Shading is for low-pass-filtered annual mean (August–July) SST (ref. 25; °C) for 1857–2007. Contours are for November–April 250 hPa wind speed (contoured interval is 2 m s$^{-1}$; negative values dashed). **b**, For November–April data, shading is for 850-hPa geopotential height, and arrows are for 850-hPa wind velocity (scale arrow at lower right indicates a 3 m s$^{-1}$ anomaly). Atmospheric fields in both panels are from the Twentieth-Century Reanalysis Project 1871–2007.

anomalies in the eastern centre of action are relatively weak (off the west coast of North America, Fig. 2a). We thus compare the $\delta^{18}O$ record with standardized low-pass-filtered (30-year cutoff) SST anomalies from the Kuroshio Extension region[25] and observe a strong positive correlation ($r = 0.72, p < 0.001$) from AD 1857 to 2007 (Supplementary Fig. S7), accounting for more than half the variance in $\delta^{18}O$.

Anomalously high SSTs in the Kuroshio Extension provide heat fluxes that generate an atmospheric wave, shifting the jet stream north over the western Pacific and south over the eastern Pacific[24] (Fig. 2a). The same wave pattern is visible lower in the atmosphere where moisture is transported (~850 hPa) as a ridge over the western Pacific and a trough over the eastern Pacific (Fig. 2b). The troughing over the eastern Pacific is conducive to mid-latitude cyclones travelling equatorward where they tap into $^{18}O$-enriched moisture over the tropical Pacific. The overall tendency for a southwesterly fetch is indicated by the 850-hPa velocity anomalies directed towards the study site (Fig. 2b). Without the warm

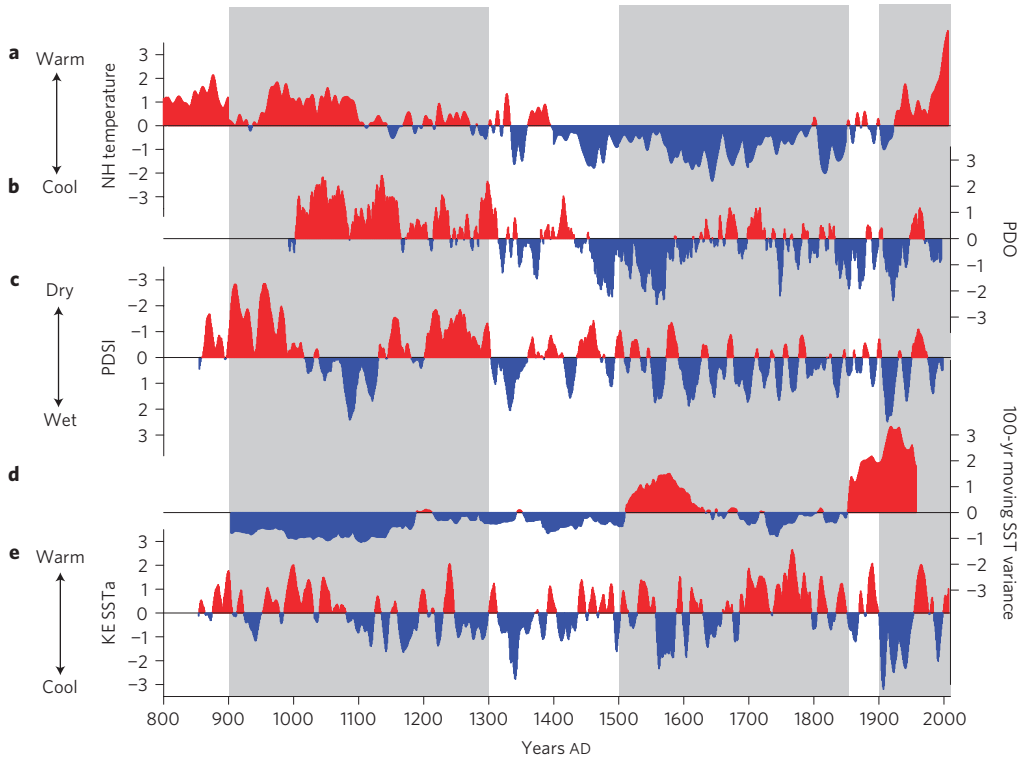


**Figure 3 | Comparison of the Kuroshio Extension SST anomaly *z*-scores with other key records. a**, Northern Hemisphere (NH) temperatures[9]. **b**, PDO Index AD 993–1996[17]. **c**, Averaged PDSI for grid sites 48, 60, 61, 73 and 74 (ref. 1). **d**, 100-year moving variance for Kuroshio Extension SST Index. **e**, Reconstructed Kuroshio Extension SST anomalies. Northern Hemisphere temperature, PDO and PDSI data are 11-year moving averages. Shaded bars denote the MCA, the LIA and the twentieth century.

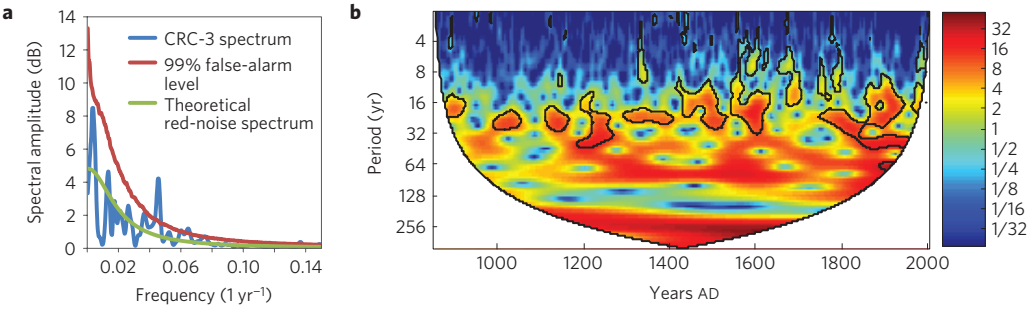


**Figure 4 | Spectral and wavelet analysis of the CRC-3 $\delta^{18}$O record. a**, Spectrum of CRC-3 $\delta^{18}$O time series estimated with a Lomb–Scargle Fourier Transform for unevenly spaced data[27]. Three overlapping segments (50%) and a Hanning window were used. Results indicate a significant peak at 22 years (99% confidence level). **b**, Continuous wavelet power spectrum (Morlet wavelet) of the CRC-3 $\delta^{18}$O record[28]. The black lines show the 5% significance level using the red noise model and the cone of influence. Results show significant periodicity in the 10–30-year band (centred at ~22). In addition, high multi-decadal power (~30–80 year band) is apparent between AD ~1300–1600 and AD 1800–2000.

Kuroshio Extension anomalies, the jet stream lacks the amplified wave structure and the flow is more zonal, allowing the incoming systems to remain more poleward and transport $^{18}$O-depleted moisture from higher latitudes.

The strong correlation between speleothem $\delta^{18}$O and Kuroshio Extension SSTs allows us to develop a calibrated and verified (Supplementary Methods and Table S3) high-resolution reconstruction of Kuroshio Extension SSTs from AD 854 to 2007 (Fig. 1). The Kuroshio Extension SST reconstruction features strong decadal variability with the highest SST anomaly (0.41 °C) occurring in AD 1765 and the lowest (−0.44 °C) in AD 1903, similar to the timing of extreme ENSO–PDO climate swings (AD 1750 and 1905) observed in some tree-ring records[16]. Taken as a whole, the mean SST anomalies are similar throughout the MCA (AD 900–1,300 =0.03 °C), Little Ice Age (LIA; 1,500–1, 850 = 0.07 °C) and the twentieth century (20th = 0.05 °C). A previous comparison with drought records from western North America showed that although most droughts occurred during periods of cool EEP SSTs, certain droughts were synchronous with warm EEP SSTs (El Niño-like) and thus required other explanations[11]. The Kuroshio Extension SST reconstruction further supports this interpretation. For instance, the record shows predominantly warm Kuroshio Extension SSTs during MCA droughts from AD ~854–1080 (Fig. 3) when EEP SSTs were warm[11], suggesting that some droughts could be driven more by NPDV than ENSO. Interestingly, the warmest Kuroshio Extension SSTs occurred during the LIA, from ~1,700 to 1,800, and the coolest occurred during the early twentieth century, a time in which SWNA was wetter than any other period of the past ~1,000 years[1,26]. The reconstructed Palmer Drought Severity Index[1] (PDSI) from grid points near the study site (Fig. 3c) indicates that

droughts occurred during periods of both warm and cool Kuroshio Extension SSTs and perhaps during positive and negative PDO (Fig. 3b), although this is dependent on which PDO reconstruction is used[17]. Therefore, this indicates that multiple factors are necessary to fully explain SWNA drought variability and highlights the need for further records to determine the mechanisms underlying North American droughts.

Spectral[27] and wavelet analyses[28] of the reconstructed SST record indicate a strong and persistent 22-year periodicity (Fig. 4), similar to the twentieth-century PDO record[7] and numerous tree-ring reconstructions[16,17], suggestive of the Hale solar cycle. Modelling studies suggest that the small solar irradiance signal may be amplified by changes in stratospheric heating or associated cloud feedbacks, both of which could influence the position of the jet stream[6,29] and therefore, the source of moisture reaching the study site. An increase in low-frequency variance, which is also seen in other records[7], becomes apparent from ~1,850 to the present (Fig. 4b). A plot of running variance shows the lowest values during the MCA (AD ~850–1100) and the highest values during the twentieth century (Fig. 3d), suggesting that NPDV may itself be affected by anthropogenic climate change rather than simply superimposed on the global-warming-related drying trend (Fig. 3a). The ensemble of 24 Intergovernmental Panel on Climate Change AR4 models is inconsistent with regard to variance change in either the PDO or North Pacific Gyre Oscillation, although the ensemble mean does suggest decreased twenty-first century variance in both modes[13].

The severity of future drought in the highly populated SWNA will undoubtedly reflect the combined influence of anthropogenic climate change and natural variability[12]. Improved understanding of the mechanisms of natural NPDV is critical for accurate predictions of future hydroclimate. This new reconstruction is the first high-resolution record of Kuroshio Extension SSTs over the past millennium and provides evidence for variable North Pacific influence on past droughts in SWNA. In addition, the record contains evidence for recent changes in NPDV, perhaps in response to rising greenhouse gases, and highlights the importance of generating new and consistent SST reconstructions to determine how various climate modes contributed to past climate variability in SWNA. This record will provide valuable data for models to further investigate the ocean–atmosphere dynamics underlying NPDV, leading to improved predictions of future hydroclimate in SWNA.

## Methods

The CRC-3 stalagmite was collected from beneath an active drip in a small isolated chamber of Crystal Cave in Sequoia National Park in 2008. The sample was cut in half, parallel to the growth axis and polished. Subsamples (~100 mg) were drilled along the growth axis for $^{230}$Th dating at the Minnesota Isotope Laboratory on a multiple-collector inductively coupled plasma mass spectrometer (Thermo-Finnigan Neptune). Corrected $^{230}$Th ages assume an initial $^{230}$Th/$^{232}$Th atomic ratio of $8 \pm 1 \times 10^{-5}$. A total of 10 $^{230}$Th dates were obtained with typical uncertainties in age (2-sigma) less than 0.1 kyr, which include analytical errors and uncertainties in the initial $^{230}$Th/$^{232}$Th ratios. Subsamples for stable isotope analysis were micromilled with a New Wave Research Micromill at 50 μm resolution for the upper 2 mm and 100 μm intervals for the remainder of the sample. The $\delta^{18}$O values of 30–70 μg powdered calcite samples were determined using a Kiel IV-carbonate device coupled with a Thermofinnigan Delta V Plus isotope ratio mass spectrometer. A total of 16 standards (NBS-19, NBS-18 and OX, an in-house quality control standard) were analysed during each run of 30 unknown samples. The results of isotopic analysis are presented in conventional delta ($\delta$) notation, defined as $\delta^{18}O = (^{18}O/^{16}O)_{sample}/(^{18}O/^{16}O)_{VPDB} - 1] * 1{,}000‰$. The standard deviation of repeated NBS-19 measurements is ~0.06‰ for $\delta^{18}$O. The raw $\delta^{18}$O and age data are presented in Supplementary Table S1. For wavelet analyses and all correlations, data were interpolated to an annual timescale using Matlab interp1 function.

Statistical analyses were conducted using JMP software. All time series and residuals from linear or multiple regressions were checked for normal distributions using the Shapiro–Wilk $W$-test. All reported correlation coefficients are Pearson's $r$ values. Spearman's $\rho$ values were also calculated and were similar to $r$ values in all cases. Significance testing was conducted using a combination of 1,000 Monte Carlo iterations and time-series modelling in the frequency domain to account for autocorrelation effects using the Matlab package of ref. 30.

**Data.** All speleothem oxygen isotope data reported in this study have been archived with the NOAA National Climatic Data Center for Paleoclimatology as McCabe-Glynn *et al.* Crystal Cave, California 1150 Year d18O Data and SST Reconstruction (ftp://ftp.ncdc.noaa.gov/pub/data/paleo/speleothem/northamerica/usa/california/crystal2013.txt).

Received 19 December 2012; accepted 29 May 2013; published online 7 July 2013

## References


1. Cook, E. R., Seager, R., Cane, M. A. & Stahle, D. W. North American drought: Reconstructions, causes, and consequences. *Earth-Sci. Rev.* **81,** 93–134 (2007).
2. McCabe, G. J., Palecki, M. A. & Betancourt, J. L. Pacific and Atlantic Ocean influences on multidecadal drought frequency in the United States. *Proc. Natl Acad. Sci. USA* **101,** 4136 (2004).
3. Dettinger, M. D., Cayan, D. R., Diaz, H. F. & Meko, D. M. North–south precipitation patterns in western North America on interannual-to-decadal timescales. *J. Clim.* **11,** 3095–3111 (1998).
4. Cook, B. I., Cook, E. R., Anchukaitis, K. J., Seager, R. & Miller, R. L. Forced and unforced variability of twentieth century North American droughts and pluvials. *Clim. Dyn.* **37,** 1097–1110 (2011).
5. Qiu, B. Interannual variability of the Kuroshio Extension system and its impact on the wintertime SST field. *J. Phys. Oceanogr.* **30,** 1486–1502 (2000).
6. Shindell, D., Rind, D., Balachandran, N., Lean, J. & Lonergan, P. Solar cycle variability, ozone, and climate. *Science* **284,** 305–308 (1999).
7. Mantua, N. J. & Hare, S. R. The Pacific decadal oscillation. *J. Oceanogr.* **58,** 35–44 (2002).
8. Cobb, K. M., Charles, C. D., Cheng, H. & Edwards, R. L. El Nino/Southern Oscillation and tropical Pacific climate during the last millennium. *Nature* **424,** 271–276 (2003).
9. Mann, M. E. *et al.* Global signatures and dynamical origins of the Little Ice Age and Medieval Climate Anomaly. *Science* **326,** 1256–1260 (2009).
10. Cole, J., Overpeck, J. & Cook, E. Multiyear La Niña events and persistent drought in the contiguous United States. *Geophys. Res. Lett.* **29,** 1647 (2002).
11. Conroy, J. L., Overpeck, J. T., Cole, J. E. & Steinitz-Kannan, M. Variable oceanic influences on western North American drought over the last 1200 years. *Geophys. Res. Lett.* **36,** L17703 (2009).
12. Seager, R. & Vecchi, G. A. Greenhouse warming and the 21st century hydroclimate of southwestern North America. *Proc. Natl Acad. Sci. USA* **107,** 21277–21282 (2010).
13. Furtado, J. C., Di Lorenzo, E., Schneider, N. & Bond, N. A. North Pacific decadal variability and climate change in the IPCC AR4 models. *J. Clim.* **24,** 3049–3067 (2011).
14. Shakun, J. D. & Shaman, J. Tropical origins of North and South Pacific decadal variability. *Geophys. Res. Lett.* **36,** L19711 (2009).
15. Latif, M. & Barnett, T. P. Causes of decadal climate variability over the North Pacific and North America. *Science* **266,** 634–637 (1994).
16. Biondi, F., Gershunov, A. & Cayan, D. R. North Pacific decadal climate variability since 1661. *J. Clim.* **14,** 5–10 (2001).
17. MacDonald, G. M. & Case, R. A. Variations in the Pacific Decadal Oscillation over the past millennium. *Geophys. Res. Lett.* **32,** L08703 (2005).
18. D'Arrigo, R. & Wilson, R. On the Asian expression of the PDO. *Int. J. Climatol.* **26,** 1607–1617 (2006).
19. Kipfmueller, K. F., Larson, E. R. & George, S. S. Does proxy uncertainty affect the relations inferred between the Pacific Decadal Oscillation and wildfire activity in the western United States? *Geophys. Res. Lett.* **39,** L04703 (2012).
20. Friedman, I., Smith, G. I., Gleason, J. D., Warden, A. & Harris, J. M. Stable isotope composition of waters in southeastern California. 1: Modern precipitation. *J. Geophys. Res.* **97,** 5795–5812 (1992).
21. Berkelhammer, M., Stott, L., Yoshimura, K., Johnson, K. & Sinha, A. Synoptic and mesoscale controls on the isotopic composition of precipitation in the western United States. *Clim. Dynam.* **38,** 433–454 (2012).
22. Scholz, D. & Hoffmann, D. L. StalAge-An algorithm designed for construction of speleothem age models. *Quat. Geochronol.* **6,** 369–382 (2011).
23. Genty, D. & Massault, M. Carbon transfer dynamics from bomb $^{14}$C and $\delta^{13}$C time series of a laminated stalagmite from SW France; modelling and comparison with other stalagmite records. *Geochim. Cosmochim. Acta* **63,** 1537–1548 (1999).
24. Ren, X., Zhang, Y. & Xiang, Y. Connections between wintertime jet stream variability, oceanic surface heating, and transient eddy activity in the North Pacific. *J. Geophys. Res.* **113,** D21119 (2008).
25. Kaplan, A. *et al.* Analyses of global sea surface temperature 1856–1991. *J. Geophys. Res.* **103,** 567–518 (1998).
26. Woodhouse, C. A., Meko, D. M., MacDonald, G. M., Stahle, D. W. & Cook, E. R. A 1,200-year perspective of 21st century drought in southwestern North America. *Proc. Natl Acad. Sci. USA* **107,** 21283–21288 (2010).

27. Schulz, M. & Mudelsee, M. REDFIT: Estimating red-noise spectra directly from unevenly spaced paleoclimatic time series. *Comput. Geosci.* **28,** 421–426 (2002).
28. Torrence, C. & Compo, G. P. A practical guide to wavelet analysis. *Bull. Am. Meteorol. Soc.* **79,** 61–78 (1998).
29. Meehl, G. A., Washington, W. M., Wigley, T. M. L., Arblaster, J. M. & Dai, A. Solar and greenhouse gas forcing and climate response in the twentieth century. *J. Climate* **16,** 426–444 (2003).
30. Macias-Fauria, M., Grinsted, A., Helama, S. & Holopainen, J. Persistence matters: Estimation of the statistical significance of paleoclimatic reconstruction statistics from autocorrelated time series. *Dendrochronologia* **30,** 179–187 (2012).

## Acknowledgements

We would like to thank the Sequoia National Park staff, especially J. Despain, A. Esperanza, B. Tobin, H. Veercamp, E. Meyer and K. Nydick. All samples were collected with permission from the National Park Service (NPS Permits: SEKI-2007-SCI- 0024, SEKI-2008-SCI-0017, SEKI-2009-SCI-0004, SEKI-2010-SCI-0060, SEKI-2011-SCI-0053 and SEKI-2012-SCI-0440). We also thank J. Southon for assistance with radiocarbon dating. This work was partly supported by a faculty seed grant from the Newkirk Center for Science and Society at the University of California, Irvine, by the National Science Foundation grants to A.S. (ATM: 0823554 and AGS: 1103360) and by NSFC grant 41230524 to H.C.

## Author contributions

A.S. initiated the project. K.R.J., A.S. and S.M-G. collected the sample and conducted the modern calibration study. H.C. and R.L.E. conducted the U-series dating. S.M-G. conducted microsampling, stable isotope analysis, and age modelling in the laboratory of K.R.J. C.S. analysed reanalysis data and identified the relationship with Kuroshio Extension SST anomalies. M.B. conducted backtracking trajectory analysis. K.R.J. and S.M-G. conducted statistical, time-series and wavelet analysis and wrote the manuscript with contributions from all authors.

## Additional information

Supplementary information is available in the online version of the paper. Reprints and permissions information is available online at www.nature.com/reprints. Correspondence and requests for materials should be addressed to K.R.J.

## Competing financial interests

The authors declare no competing financial interests.